SANDIA REPORT
SAND2010-7250
Unlimited Release
Printed September 2010

Influence of Point Defects on Grain Boundary Motion

Stephen M Foiles

Prepared by
Sandia National Laboratories
Albuquerque, New Mexico 87185 and Livermore, California 94550

Sandia National Laboratories is a multi-program laboratory managed and operated by Sandia Corporation, a wholly owned subsidiary of Lockheed Martin Corporation, for the U.S. Department of Energy's National Nuclear Security Administration under contract DE-AC04-94AL85000.

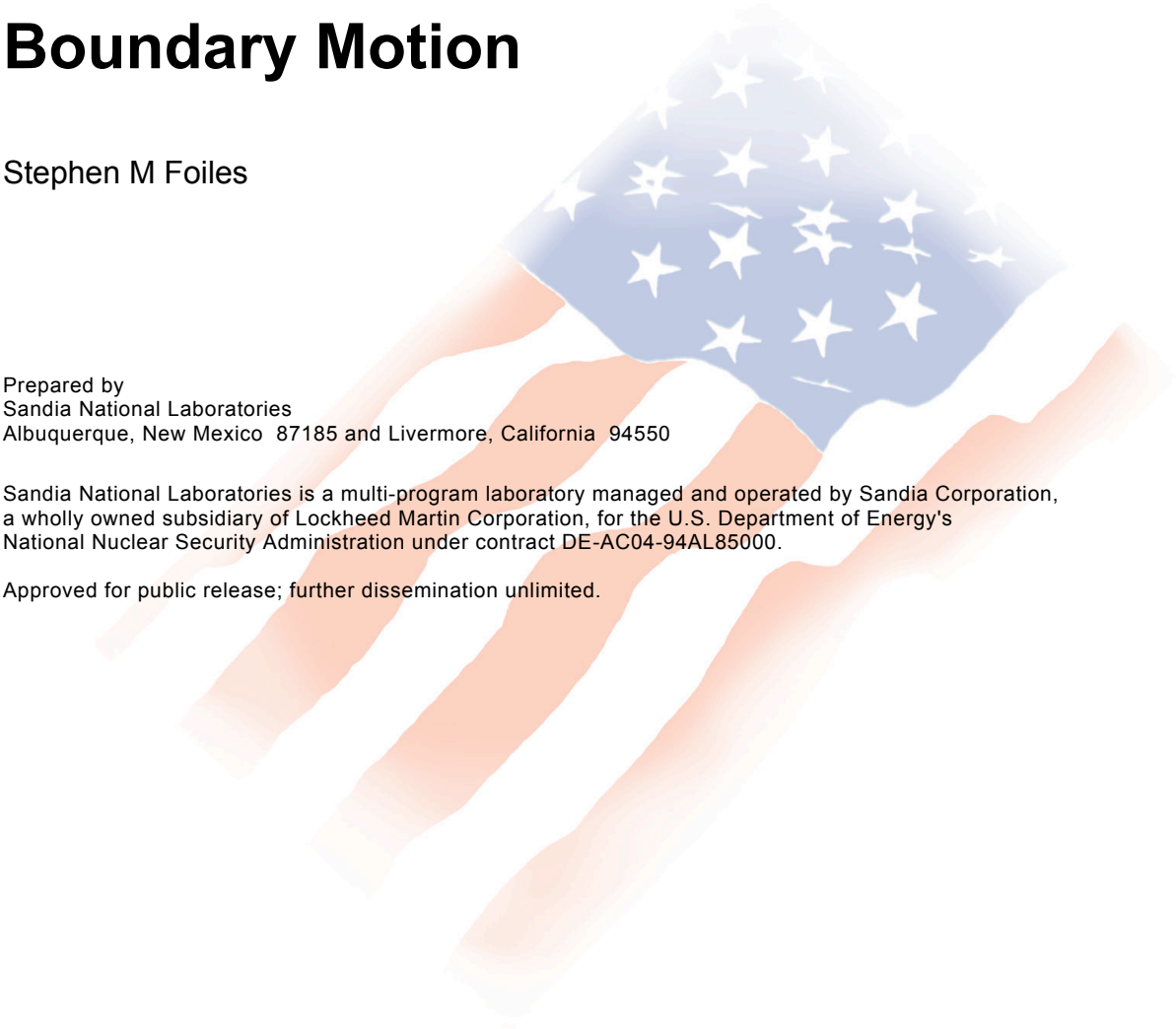

Issued by Sandia National Laboratories, operated for the United States Department of Energy by Sandia Corporation.

Available to DOE and DOE contractors from
U.S. Department of Energy
Office of Scientific and Technical Information
P.O. Box 62
Oak Ridge, TN 37831

Telephone: (865) 576-8401
Facsimile: (865) 576-5728
E-Mail: reports@adonis.osti.gov
Online ordering: http://www.osti.gov/bridge

Available to the public from
U.S. Department of Commerce
National Technical Information Service
5285 Port Royal Rd.
Springfield, VA 22161

Telephone: (800) 553-6847
Facsimile: (703) 605-6900
E-Mail: orders@ntis.fedworld.gov
Online order: http://www.ntis.gov/help/ordermethods.asp?loc=7-4-0#online

SAND2010-7250
Unlimited Release
Printed September 2010

Influence of Point Defects on Grain Boundary Motion

Stephen M Foiles
Computational Materials Science and Engineering Department
Sandia National Laboratories
P.O. Box 5800
Albuquerque, New Mexico 87185-MS1411

Abstract

This work addresses the influence of point defects, in particular vacancies, on the motion of grain boundaries. If there is a non-equilibrium concentration of point defects in the vicinity of an interface, such as due to displacement cascades in a radiation environment, motion of the interface to sweep up the defects will lower the energy and provide a driving force for interface motion. Molecular dynamics simulations are employed to examine the process for the case of excess vacancy concentrations in the vicinity of two grain boundaries. It is observed that the efficacy of the presence of the point defects in inducing boundary motion depends on the balance of the mobility of the defects with the mobility of the interfaces. In addition, the extent to which grain boundaries are ideal sinks for vacancies is evaluated by considering the energy of boundaries before and after vacancy absorption.

ACKNOWLEDGMENTS

The Laboratory Directed Research and Development (LDRD) program at Sandia National Laboratories supported this work

CONTENTS

FIGURES

NOMENCLATURE

MD	Molecular Dynamics
EAM	Embedded Atom Method
SI	Self-interstitial
SFT	Stacking Fault Tetrahedra
LAMMPS	Large Atomic/Molecular Massively Parallel Simulator
DOE	Department of Energy
SNL	Sandia National Laboratories

1. INTRODUCTION

Understanding and controlling the evolution of materials microstructure, including grain size, is key to the development and evaluation of novel materials especially in extreme environments. This in turns requires a quantitative understanding of the mobility of the grain boundaries as well as an understanding of the various driving forces that cause grain boundary motion. We have recently completed an extensive study of boundary mobility in the absence of crystalline defects [1]. However, boundary motion can be driven by a difference in the defect energy density on the two sides of the boundary. This is relevant to the metallurgical phenomena of recrystallization and also to the evolution of microstructures in a radiation environment. In the latter case, displacement cascades can produce large point defect densities that can be locally inhomogeneous and so cause boundary motion. The goal of this proposal is to perform the first evaluation of the mobility of grain boundaries driven by a difference in point defect densities across the boundary. This is directly relevant to grain boundary motion due to radiation damage. It also addresses a long-standing question as to whether grain boundary mobilities associated with curvature driven growth are the same as the mobilities in defect driven growth such as in recrystallization.

Simulations of grain boundary mobility have mainly occurred in the last decade since it is computationally intensive. A variety of simulation methods have been employed that correspond to different driving forces for the motion. The driving forces considered to date include curvature driven[2], elastic strain driven[3], synthetic driving forces[1, 4] and non-driven (fluctuation-based) methods[5, 6]. To date, motion driven by differences in defect densities between the adjoining crystals have not been considered. This class of driving forces is relevant to recrystallization phenomena, where an essentially defect-free grain grows at the expense of highly deformed, and so defected, grains. The current project focuses on one aspect of such defect-driven motion, point defect driven motion.

This problem is also of direct relevance to grain motion in radiation-damaged materials. There have been some preliminary molecular dynamics studies of the influence of displacement cascades on nearby boundaries [7-10]. These studies have observed changes in the boundary structure and what appears to be boundary motion induced by the presence of a high-density of vacancies and self-interstitials. However, these observations do not allow the separation of the influence of the two types of point defects on the boundary motion. In addition, the creation of a displacement cascade provides a local heating of the region. This will also influence the motion of grain boundaries. The current study will focus on the influence of vacancies on adjacent grain boundaries. This work will assist in unraveling the various effects that could occur in the case of radiation damage.

2. SIMULATION METHODOLOGY

This study employs direct molecular dynamics (MD) simulations of the motion of two specific grain boundaries in the presence of a non-equilibrium concentration of vacancies. The dynamics of the system will be followed by standard molecular dynamics techniques. The evolution of the system will be visualized by techniques that allow for the location of the grain boundary and the identification of the vacancies. This motion will then be analyzed to obtain insight into the questions presented above.

The MD simulations were performed using the LAMMPS [11] code. The MD computational cell has periodic boundary conditions in all three directions. Two grain boundaries of opposite sense are present in the cell and oriented normal to the long direction of the cell. The simulations are performed in the isothermal-isobaric (NPT) ensemble. This allows the cell length to adjust in response to the possible change in the number of vacancies during the course of the simulation. The interatomic potentials employed are of the embedded-atom-method (EAM) [12] type. The specific potentials used were developed by Foiles and Hoyt [5] to model Ni. These potentials have been used in other studies of grain boundary energy and motion [1, 5, 13-15].

The motion of the grain boundary is tracked using a method used in previous MD studies of interfacial kinetics [5, 16]. The location of the interface is determined by associating with each atom a local order parameter which reflects whether the local environment is closer to crystal A or closer to crystal B. In particular, the parameter p_i is defined by $p_i = \sum_j \left(\vec{R}_{ij} - \vec{R}_j^A\right)^2 - \sum_j \left(\vec{R}_{ij} - \vec{R}_j^B\right)^2$. In this expression, j refers to the 12 nearest neighbors of atom I, $\vec{R}_{ij}$ is the vector from the atom I to atom j, and $\vec{R}_j^A$ denotes the nearest neighbor vectors in the ideal crystal A and similarly for B. In each case, the order of the assignment of the neighbor atoms j is such as to minimize each sum. This parameter will be an approximately constant negative value in crystal A and a corresponding positive value in crystal B. In a region that does not correspond to either crystal, the value will average about zero. The average position of the grain boundaries are obtained by averaging the values of this parameter over planes parallel to the boundaries. The point where this average crosses zero is taken as the average position of the grain boundary.
Determining the coordination number of each atom identifies vacancies. A cluster of 12 under-coordinated atoms surrounds the vacancy. Under-coordinated atoms can occur in other situations, in particular, in the grain boundary. However. The pattern of the cluster around the vacancy provides a clear signature.

Two grain boundaries were selected for this study based on their relatively high mobility. Olmsted , *et al.* [1] determined the mobility of a set of 388 grain boundaries. Two boundaries with high mobility were studied; the boundaries number 47 and 80 in the supplemental data that will be referred to here as boundaries A and B, respectively. The complete specification of the boundaries can be found there. Both boundaries are Σ3 boundaries and so have the same misorientation between the crystals, but with different boundary normals. Boundary A has <6 2 2> boundary normals while boundary B has <3 2 1> boundary normals. The MD simulation cells are constructed so that the boundaries are initially about 10 nm apart and have boundary

areas of about 40 and 45 nm^2. The numbers of atoms in the simulations cells are 86007 for boundary A and 66524 for boundary B.

3. RESULTS

3.1 Bulk Vacancy Properties

The simulations performed are start with a non-equilibrium concentration of vacancies. It is useful to know the properties of these vacancies predicted by these potentials. The vacancy formation energy for these potential is 1.76 eV [5]. The kinetics of the motion of an existing vacancy is governed by the vacancy migration activation energy. This has been computed here using standard techniques to be E^m = 0.88 eV. Thus the total activation energy for vacancy diffusion, Q, is 2.64 eV.

For the present simulation, we can estimate the rate of vacancy hops in the bulk using E^m. The hopping rate for individual vacancies should be approximated by $\nu_{hop} = \nu_0 e^{-E^m/k_B T}$. In this expression, ν_0 is a characteristic vibration frequency that will be approximated by the Debye frequency of Ni, $\nu_0 = 8 \times 10^{12} s^{-1}$. This translates to estimates of the bulk vacancy hopping frequencies of 0.06/ns, 0.7/ns and 4/ns for the three temperatures of 0.55, 0.70 and 0.85 T_M, respectively. Since the present simulations are run for 10 ns, one would expect to see only limited motion of the bulk vacancies at the lowest temperature, but significant motion of the bulk vacancies at the highest temperature. This is consistent with the visualization of the simulation results.

It is also relevant to evaluate the equilibrium vacancy concentrations at the simulation temperatures. The equilibrium concentration will be given by $c_v = e^{-E_v^f/k_B T}$. Given the vacancy formation energy quoted above, this gives equilibrium vacancy concentrations of 5×10^{-11}, 8×10^{-9}, and 2×10^{-7}, at the reduced temperatures of 0.55, 0.70 and 0.85, respectively. Thus for the simulation cells used in this study, the equilibrium number of bulk vacancies is significantly less than 1.

3.2 Mobility of Boundaries in the Absence of Vacancies

As a precursor to the analysis of the influence of the presence of vacancies on the boundary motion, the mobility of these boundaries was determined in the absence of vacancies. Te mobility was determined using a method described by Trautt, *et al* [6]. In this approach, the average position of the boundary, h(t), is monitored as a function of time. The mobility is then related to the mean squared displacement of via the equations $\left\langle \left(h(\tau + t) - h(\tau) \right)^2 \right\rangle = Dt$ and $D = \frac{2Mk_B T}{A}$. In these expressions, M is the boundary mobility, A is the area of the boundary in the simulation cell and the angle brackets refer to an average over τ. The mean square displacement as a function of time is plotted in Figure xx. Note that one obtains the expected linear behavior albeit with a fair amount of statistical noise. It is also important to note that the variation with temperature is of these curves is the opposite for the two boundaries. The inferred mobility values are presented in Figure xxc. The values of the higher temperature mobilities are

similar to those found at somewhat different temperatures and by a different method [4] by Olmsted, Holm and Foiles [1].

An important observation about these mobility values is that the temperature dependence of the mobility is totally different for the two different boundaries. It is usually assumed that grain boundary motion is an activated process and so the mobility is assumed to follow Arrhenius behavior [17]. The behavior of boundary B is roughly in accord with this expectation, thought the Arrhenius plot is not particularly linear. Boundary A is seen to have higher mobility at lower temperatures. Olmsted, Holm ad Foiles [1] saw such behavior earlier. The variation of boundary mobility with temperature is a topic that deserves further study.

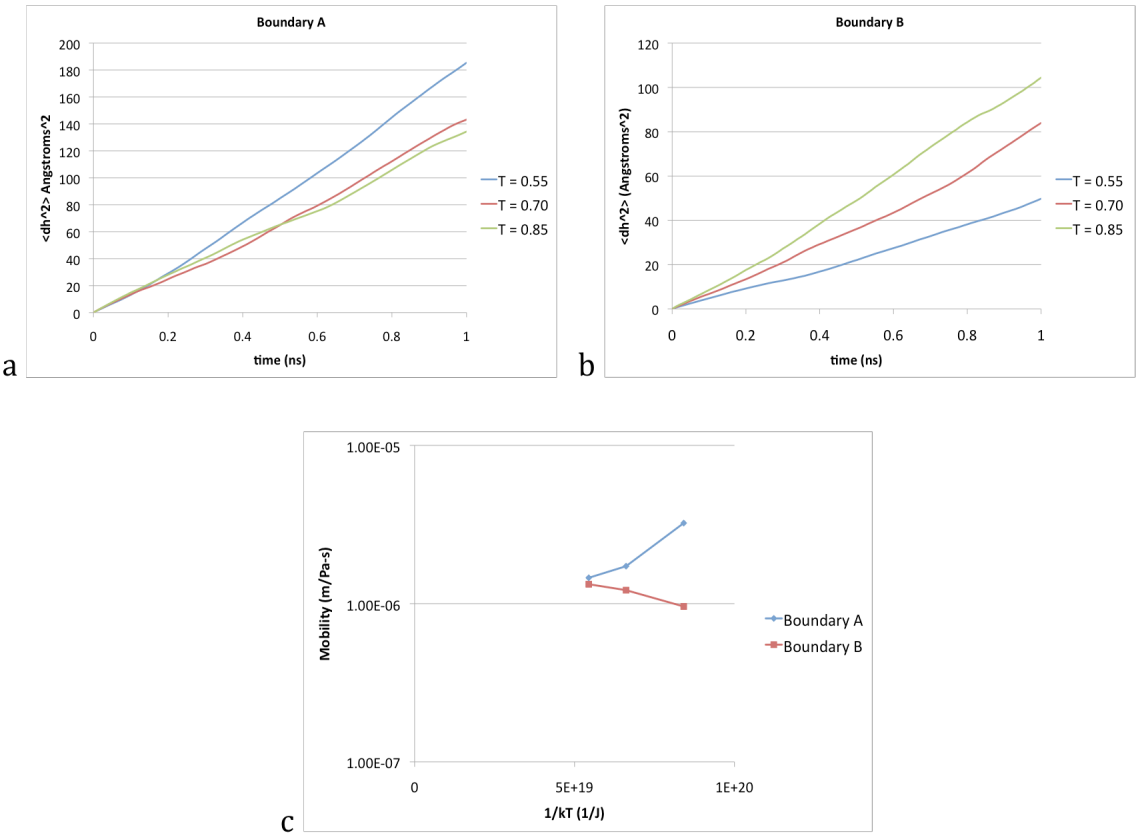

Figure 1. The mean squared displacement (see text) as a function of time for boundary A (a) and B (b) and the inferred mobility of these boundaries in (c).

3.3 Influence of Vacancies on Boundary Motion

Simulations were performed in which there is a significant vacancy concentration on one side of a grain boundary. These simulations are intended to provide a qualitative understanding of the influence of the presence of such an arrangement. The vacancy concentration is produced as follows. The cell contains two grain boundaries with opposite misorientations in the periodic

cell. In the region between the two boundaries in the center of the cell, vacancies are created on 02% of the lattice sites. This produces an arrangement where each boundary has no vacancies on one side and a concentration of 0.2% vacancies on the other. If one assumes that the vacancies will pull the boundaries toward them in order to eliminate the vacancies, then the two boundaries will move towards each other.

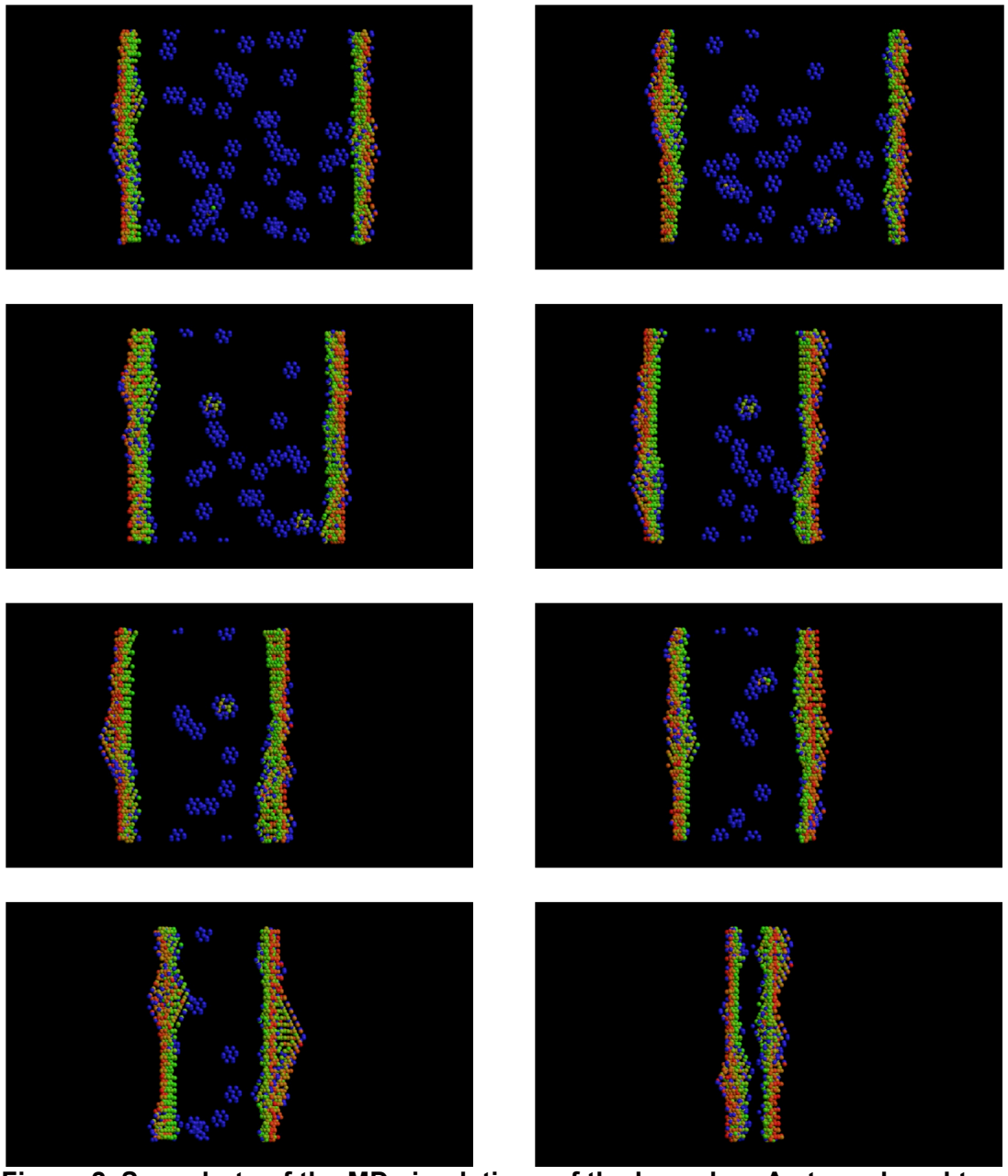

Figure 2. Snapshots of the MD simulations of the boundary A at a reduced temperature of 0.7 and with a 0.2% initial concentration of vacancies between the boundaries. The snapshots are at intervals of 0.25 ns. The red to green atoms are the atoms with local atomic environment intermediate to the two crystals, in other words the grain boundaries. The blue atoms are under-coordinated atoms. Each cluster of blue atoms corresponds to a vacancy.

Figure 2 shows snapshots of the evolution of boundary A for a reduced temperature of 0.70. The snapshots are at 0.25ns intervals. Note that atoms with local neighbor positions that correspond to one of the two crystals are not shown. The blue atoms are under-coordinated and the clusters of such atoms are vacancies. The atoms shaded between red and green are atoms whose local neighbor environment is intermediate between the two crystals and correspond to the grain boundaries. The behavior of this simulation is consistent with a driven motion of the boundary towards the vacancy concentration. Observation of the visualization of this simulation clearly shows that there are two processes by which the vacancies are removed from the system and therefore the overall energy of the system reduced. First, the random motion of the vacancies in some cases causes them to impinge on the boundary and to be absorbed. The other process is the motion of the boundary that sweeps out vacancies. This latter process gives an energetic advantage to motion into regions of high defect concentration and so can bias the motion. These two processes are both expected and their relative contributions depend on the relative values of the vacancy mobility and the boundary mobility, both of which change with temperature. In this case, the bias of the boundary motion appears to have been sufficient to cause the boundaries to approach each other and ultimate annihilate shortly after the last frame in Figure 2.

Figure 3 shows snapshots at the corresponding simulation of boundary B except that in this case, the snapshots are separated by times of 1 ns. Note that the structure of the boundary in this case is much more diffuse than for boundary A. Also, recall that the mobility of boundary B is lower than that of boundary A. Observation of the visualization shows that in the initial phase of the simulation, that there appears to be a bias of the motion of the boundaries into the region of vacancies. During this time the vacancy concentration, though, decreases due to absorption of the vacancies at the boundary due to vacancy motion. In the latter part of the simulation, there are no longer significant numbers of vacancies within the immediate vicinity of the boundary. The motion of the boundaries then appears to be random fluctuations similar to that for the simulations with no vacancies. This suggests that the influence of vacancies on the motion of grain boundaries is very short ranged. This result is not surprising given that the long-range strain field associated with vacancies is small and so they are unlikely to influence boundary motion over significant distances.

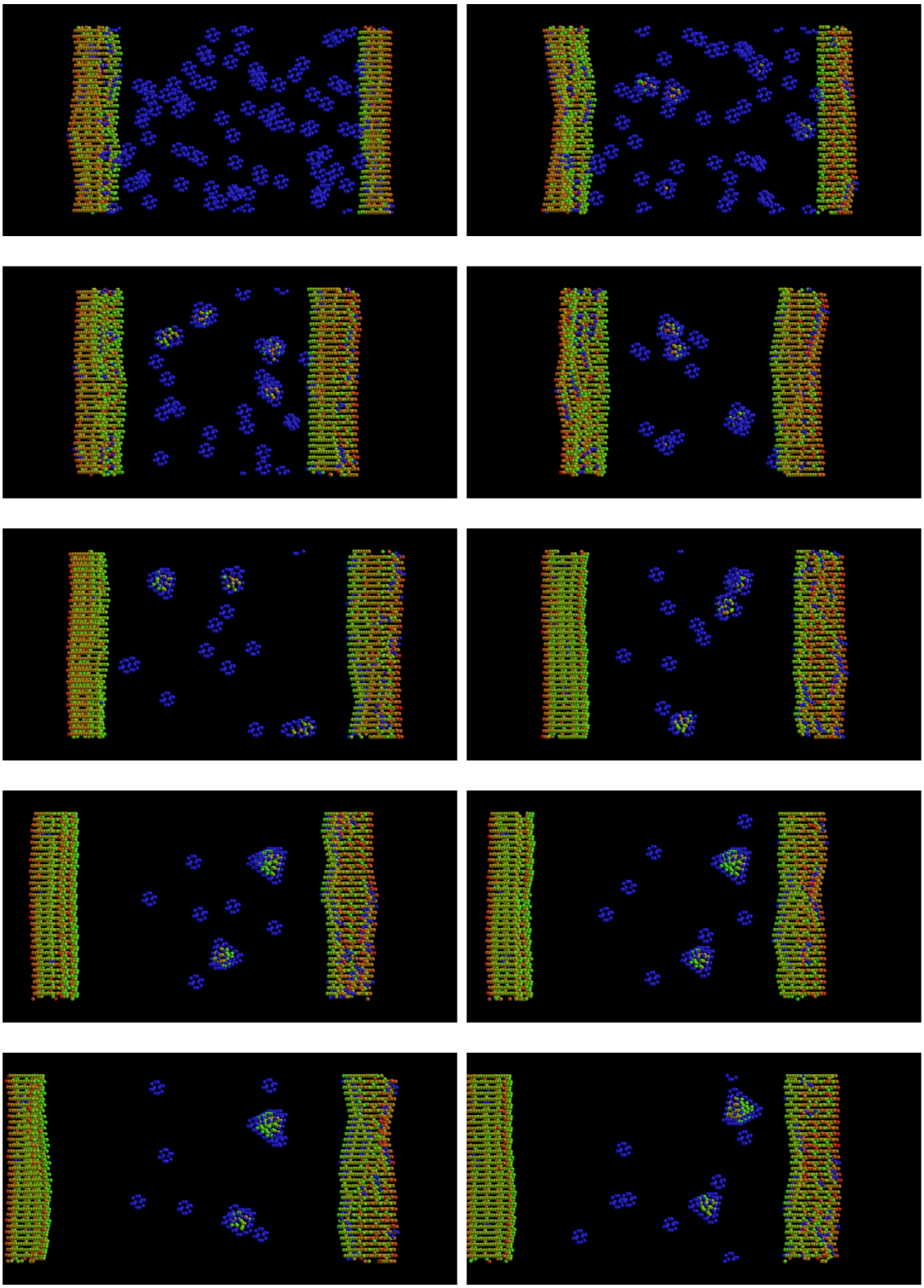

Figure 3. Same as Figure 2 expect for boundary B and the frames are at 1 ns intervals.

Simulations were also performed at a reduced temperature of 0.55 for both boundaries and the same concentration of vacancies. At this lower temperature, there is substantially less vacancy

motion on the time scale of these simulations. Most of the vacancy motion that does occur is short-range. This short-range vacancy motion does result in the formation of small stacking fault tetrahedrons (SFT). SFT's are well-known compact defect structures that form from the combination of vacancies [18]. The boundary motion observed in the visualizations can be characterized as follows. The vacancies stay in the same region. When the boundaries fluctuate into regions where there is a significant concentration of vacancies, the motion appears to be temporarily biases in that direction, but after the vacancies are absorbed, the boundaries appear to fluctuate randomly until the next fluctuation into a region of vacancies. The primary difference between the two boundaries is that the boundary motion is significant smaller for boundary B consistent with its lower mobility.

High temperature simulations where also performed at a reduced temperature of 0.85. At this temperature there is substantially greater vacancy motion consistent with the activation energies discussed above. The mobility of these boundaries, though, is not dramatically different from the simulations at a temperature of 0.70. The visualization of these simulations show that the dominant behavior is the absorption of vacancies due to their random impingement on the boundaries and apparently random modest fluctuations in the boundary position.

3.4 Evaluation of Grain Boundaries as Sinks

It is often argued that grain boundaries act as sources and sinks for vacancies and interstitials. An unanswered question is whether they are perfect sources or sinks in the sense that the properties of the grain boundary are not modified appreciably by the absorption or emission of vacancies and interstitials. Qualitatively, watching the visualization of the absorption of vacancies in this study, it appears that the grain boundaries are acting as ideal sinks. In order to evaluate this quantitatively, the grain boundary energy will be evaluated for boundaries that have absorbed significant numbers of vacancies compared to the energy of boundaries that have not absorbed vacancies.

The simulations that will be considered are those performed at a reduced temperature of T = 0.85. The reason for this choice is ease. At the high temperatures, the vacancies are mobile and they are largely absorbed by the boundaries before the grain boundaries meet and annihilate. An example of such a state is shown in Figure x that shows the simulation a grain boundary A with an initial vacancy concentration of 0.2% after evolution for 3 ns at T=0.85. One sees that the grain boundaries are well separated and that there are just 3 mono-vacancies remaining.

The energy of the two grain boundaries in the absence of vacancy absorption was computed as follows. A configuration for the simulation without vacancies at T = 0.85 was minimized. In the minimization, the area of the grain boundary was set to that appropriate to the zero-temperature lattice constant and a minimization over the length of the cell was performed. This process yields a grain boundary energy f 971 and 493 mJ/m^2 for boundaries A and B, respectively. These value will be taken as representative of the internal energy of the structure of the boundary at these high temperatures. It should be noted that these energies differ from the optimal zero-temperature energies obtained by Olmsted, *et al.* [14] of 874 and 473 mJ/m^2. While the size of this difference, especially for boundary A, is somewhat surprising, it is not unexpected that the structures that the boundary assumes at high temperatures will be different from the optimal

zero-temperature structure. This is discussed in detail by Olmsted *et al* [19] who point out that structural changes with temperature can occur in part due to the change in the elastic properties of the material at high temperatures.

The corresponding calculation of the grain boundary energy was performed for the systems with vacancies. The energy of the full system required to computed the grain boundary energy was corrected for the extra energy associated with the remaining vacancies. For the case of boundary A, the energy was computed at 2.4 ns when there were 8 isolated vacancies remaining in the system out of the initial 65. The grain boundary energy obtained was 1024 mJ/m^2. It was also computed for the system at 3ns with 3 remaining vacancies and energy of 1015 mJ/m^2 was obtained. Both of these energies are higher than the case without vacancy absorption by about 5%. This suggests that the process of vacancy absorption has slightly increased the energy, though it is interesting to note that the absorption of the last 5 vacancies actually led to a somewhat lower energy. For boundary B, the energy was calculated at 7.3 ns into the run and with a single vacancy present. The grain boundary energy obtained in that case was 509 mJ/m^2, about 3% higher.

4. SUMMARY AND FUTURE DIRECTIONS

This study has looked at the influence on grain boundary motion of the interaction of a high concentration of vacancies in the vicinity of the grain boundary. The current study is only qualitative. A more quantitative analysis was not possible within the funding levels of this project. The results indicate that the influence of vacancies on boundary motion depends on the relative mobility of the vacancies and the grain boundary. In the limit that the boundary mobility dominates, there appears to be a short-ranged bias for motion that sweeps up the vacancies. However, if the boundary then fluctuates away from the vacancies, its subsequent motion appears random. In the limit that the vacancy mobility dominates, the vacancies are absorbed by the boundary when they impinge upon, but do not appear to induce significant boundary motion. Note that the two boundaries in the current study were chosen for their relatively high mobility, so the latter scenario is probably the more common. It was also noted that the absorption of vacancies made only modest changes in the boundary energy and did not appear to change the boundary mobility. This is consistent with the prevailing view that grain boundaries provide ideal sources/sinks for vacancies.

The present work suggests that for the previous simulation studies that reported boundary motion due to the presence of displacement cascades that the vacancies produced in the cascades are not the primary cause of the motion. This suggests future studies of the influence of self-interstitials on boundary motion. Another area of future research suggested by this study is the temperature dependence of grain boundary mobility. In this study, deviations from the generally assumed Arrhenius temperature dependence were observed. It would be important to understand the factors that control the temperature dependence of mobility.

5. REFERENCES

1. Olmsted, D., E.A. Holm, and S.M. Foiles, *Survey of computed grain boundary properties in face-centered cubic metals: II. Grain boundary mobility.* Acta Materialia, 2009. **57**: p. 3704-3713.
2. Upmanyu, M., R.W. Smith, and D.J. Srolovitz, *Atomistic SImulation of Curvature Driven Grain Boundary Migration.* Interface Science, 1998. **6**: p. 41-58.
3. Zhang, H., M.I. Mendelev, and D.J. Srolovitz, *Computer simulation of the elastically driven migration of a flat grain boundary.* Acta Materialia, 2004. **52**: p. 2569-2576.
4. Janssens, K.G.F., et al., *Computing the Mobility of Grain Boundaries.* Nature Materials, 2006. **5**: p. 124-127.
5. Foiles, S.M. and J.J. Hoyt, *Computation of Grain Boundary Stiffness and Mobility from Boundary Fluctuations.* Acta Materialia, 2006. **54**: p. 3351-3357.
6. Trautt, Z.T., M. Upmanyu, and A. Karma, *Interface Mobility from Interface Random Walk.* Science, 2006. **314**: p. 632-635.
7. Samaras, M., et al., *Computer simulation of displacement cascades in nanocrystalline Ni.* Physical Review Letters, 2002. **88**: p. 125505.
8. Samaras, M., et al., *Radiation damage near grain boundaries.* Philosophical Magazine, 2003. **83**: p. 3599.
9. Samaras, M., et al., *SIA activity during irradiation of nanocrystalline Ni.* Journal of Nuclear Materials, 2003. **323**: p. 213.
10. Voegeli, W., K. Albe, and H. Hahn, *Simulation of grain growth in nanocrystalline nickel induced by ion irradiation.* Nuclear Instruments and Methods in Physics Research B, 2003. **202**: p. 230.
11. Plimpton, S.J., *LAMMPS: Large-scale Atomic/Molecular Massively Parallel Simulator*. 2007, Sandia National Laboratories.
12. Daw, M.S., S.M. Foiles, and M.I. Baskes, *The embedded-atom method: a review of theory and applications.* Materials Science Reports, 1993. **9**: p. 251-310.
13. Holm, E.A. and S.M. Foiles, *How Grain Growth Stops: A Mechanism for Grain-Growth Stagnation in Pure Materials.* Science, 2010. **328**: p. 1138-1141.
14. Olmsted, D., S.M. Foiles, and E.A. Holm, *Survey of computed grain boundary properties in face-centered cubic metals: I. Grain boundary energy.* Acta Materialia, 2009. **57**: p. 3694-3703.
15. Olmsted, D.L., S.M. Foiles, and E.A. Holm, *Grain boundary interface roughening transition and its effect on grain boundary mobility for non-faceting boundaries.* Scripta Materialia, 2007. **57**: p. 1161-1164.
16. Hoyt, J.J., M. Asta, and A. Karma, *Method for Computing the Anisotropy of the Solid-Liquid Interfacial Free Energy.* Physical Review Letters, 2001. **86**: p. 5530.
17. Sutton, A.P. and R.W. Balluffi, *Interfaces in Crystalline Materials*. 1995, Oxford: Clarendon Press.
18. Hirth, J.P. and J. Lothe, *Theory of Dislocations*. Second Edition ed. 1982, New York: John Wiley & Sons.
19. Olmsted, D.L., et al., *Routes to Grain-Boundary Disorder in Hot Polycrystals.* Physical Review Letters, submitted.

DISTRIBUTION

1	MS0899	Technical Library	9536 (electronic copy)


Sandia National Laboratories